

# The Effects of Reactive Oxygen Species on Internodal Myelin Structure, and Role of Plasmalogen Phospholipids as Endogenous Antioxidants

Author: Adrienne M. Luoma

Persistent link: <http://hdl.handle.net/2345/1943>

This work is posted on [eScholarship@BC](http://escholarship@bc.edu),  
Boston College University Libraries.

---

Boston College Electronic Thesis or Dissertation, 2009

Copyright is held by the author, with all rights reserved, unless otherwise noted.

Boston College  
The Graduate School of Arts and Sciences  
Department of Biology

THE EFFECTS OF REACTIVE OXYGEN SPECIES ON INTERNODAL MYELIN  
STRUCTURE, AND ROLE OF PLASMALOGEN PHOSPHOLIPIDS AS  
ENDOGENOUS ANTIOXIDANTS

a thesis

by

ADRIENNE MARIE LUOMA

submitted in partial fulfillment of the requirements

for the degree of

Master of Science

May 2009

© copyright by ADRIENNE MARIE LUOMA  
2009

## Abstract

# THE EFFECTS OF REACTIVE OXYGEN SPECIES ON INTERNODAL MYELIN STRUCTURE, AND ROLE OF PLASMALOGEN PHOSPHOLIPIDS AS ENDOGENOUS ANTIOXIDANTS

By: Adrienne Marie Luoma

Advisor: Daniel A. Kirschner, Ph.D.

Reactive oxygen species (ROS) are implicated in a range of degenerative conditions, including aging, neurodegenerative diseases, and neurological disorders such as multiple sclerosis. Myelin is a lipid-rich multilamellar assembly that facilitates rapid nerve conduction in higher animals, and may be intrinsically vulnerable to oxidative damage given the high energetic demands and low antioxidant capacity of myelinating cells. To determine whether ROS can cause structural damage to internodal myelin, whole mouse sciatic and optic nerves were incubated *ex vivo* with a previously-characterized copper (Cu)/hydrogen peroxide (HP)/o-phenanthroline (OP)-based hydroxyl radical-generating system followed by quantitative determination of myelin packing by x-ray diffraction. Exposure to Cu/OP/HP-mediated ROS caused irreversible myelin decompaction in both sciatic and optic nerves. The addition of the hydroxyl radical scavenger, sodium formate, to the ROS-producing incubation solution significantly prevented sciatic nerve myelin decompaction, implicating hydroxyl radical species in causing the damage. Furthermore, Cu/OP/HP-mediated decompaction could be prevented by the addition of EDTA, which can compete with OP for Cu binding and

sequester the metal within the bulk solution. These findings suggest that Cu/OP/HP-dependent myelin decompaction is caused by OP-mediated membrane-targeted hydroxyl radical production. Myelin membranes are particularly enriched in plasmalogen phospholipids, which have been linked to antioxidant activity; this enrichment may constitute an endogenous ROS-defense mechanism that protects ROS-vulnerable myelin tissue from damage. Intriguingly, it was found that sciatic nerve myelin from plasmalogen deficient (Pex7 KO) mice was significantly more susceptible to ROS-mediated decompaction than that from WT mice, supporting the role of plasmalogens as endogenous antioxidants.

<b>Table of Contents</b>	<b>i</b>
<b>List of Tables and Figures</b>	<b>ii</b>
<b>Abbreviations</b>	<b>iv</b>
<b>Introduction</b>	<b>1</b>
<b>Materials and Methods</b>	<b>8</b>
Mice	8
Nerve incubation/ROS-generating system	8
X-ray diffraction and myelin structure analysis	9
<b>Results</b>	<b>11</b>
Sciatic nerve myelin undergoes decompaction after exposure to a membrane-targeted hydroxyl radical-generating system	11
Plasmalogen phospholipids offer sciatic nerve myelin protection from ROS-mediated decompaction	14
Effects of ROS on optic nerve myelin decompaction	17
<b>Discussion</b>	<b>19</b>
<b>Figures</b>	<b>24</b>
<b>References</b>	<b>50</b>

## Figures

<b>Figure 1.</b> Mechanism of <i>in vitro</i> ROS production.	24
<b>Figure 2.</b> Incubation of sciatic nerves with an ROS-generating system induces irreversible myelin decompaction.	26
<b>Figure 3.</b> Glutaraldehyde fixation does not change myelin packing of control or Cu/OP/HP-treated sciatic nerves.	28
<b>Figure 4.</b> Cu/OP/HP sciatic nerve treatment causes disordering and decompaction of myelin lamellae.	30
<b>Figure 5.</b> Cu/OP/HP-induced sciatic nerve myelin decompaction is mitigated by addition of a hydroxyl radical scavenger.	32
<b>Figure 6.</b> EDTA largely prevents Cu/OP/HP-mediated sciatic nerve myelin decompaction.	34
<b>Figure 7.</b> Sciatic nerve myelin from plasmalogen-deficient mice has a similar structure and stability to that from WT mice.	36
<b>Figure 8.</b> Sciatic nerve myelin from Pex7 KO mice is more vulnerable to ROS-mediated decompaction.	38
<b>Figure 9.</b> Sciatic nerve myelin from Pex7 KO mice is more vulnerable to ROS-mediated decompaction.	40
<b>Figure 10.</b> Pex7 KO sciatic nerve myelin decompaction induced by Cu/OP/HP treatment is mitigated by addition of a hydroxyl radical scavenger.	42

<b>Figure 11.</b> Pex7 KO sciatic nerve myelin decompaction induced by Cu/OP/HP treatment is mitigated by addition of a hydroxyl radical scavenger.	44
<b>Figure 12.</b> Incubation of WT optic nerves with an ROS-generating system induces irreversible myelin decompaction.	46
<b>Figure 13.</b> Additional sciatic nerve control experiments.	48



## Abbreviations

AD	Alzheimer's disease
CNS	Central nervous system
Cu	Copper (II) sulfate, CuSO <sub>4</sub>
EDTA	Ethylenediaminetetraacetic acid
Glut	Glutaraldehyde
HP	Hydrogen peroxide, H <sub>2</sub> O <sub>2</sub>
MS	Multiple sclerosis
OP	<i>o</i> -phenanthroline
OS	Oxidative stress
PB	Phosphate buffer
P0	Myelin protein zero
PBS	Phosphate-buffered saline
Pex7	Peroxisomal biogenesis factor 7
PNS	Peripheral nervous system
PUFA	Polyunsaturated fatty acid
ROS	Reactive oxygen species
SFD	Specimen-to-film distance
XRD	X-ray diffraction

## **Introduction**

There are certain perils associated with having an aerobic metabolism, as 1-3% of the oxygen we breathe is converted to the superoxide radical anion by incomplete mitochondrial oxygen reduction (Halliwell and Gutteridge, 2007). The discovery of the enzymes superoxide dismutase and catalase, which have evolved to catalyze the reduction of superoxide to hydrogen peroxide and the dismutation of hydrogen peroxide (HP), respectively, demonstrates the potential toxicity of these reactive oxygen species (McCord and Fridovich, 1969). The condition in which the production of reactive oxygen species (ROS) exceeds an organism's ability to scavenge these is dubbed "oxidative stress" (OS), and chronic oxidative stress has been linked to many different degenerative conditions, as well as aging itself (Stadtman, 1992).

Oxidative stress had been linked to pathology in a myriad of diseases, and the relationship between OS and the progression of neurodegenerative diseases is particularly strong (Halliwell, 1994). Post-mortem analyses of Alzheimer's disease (AD) patients have revealed the presence of oxidative damage to brain proteins and lipids, in addition to an OS-induced elevation in the cellular antioxidant systems (Huang, Moir, et al., 2004). The brain areas most loaded with the toxic A $\beta$  peptide closely correlate with those regions containing heightened lipid peroxidation, suggesting a role of oxidative damage in this pathology (Lovell, Ehmman, et al., 1995). The pathology of the demyelinating neuroinflammatory disease multiple sclerosis (MS) also correlates with oxidative damage. Examination of MS lesion sites has revealed an increase in carbonyl degradation products resulting from lipid acyl chain degradation in comparison from normal age-matched

controls (LeVine and Wetzel, 1998). The abundance of lipid peroxidation products within lesion sites suggests that oxidative damage may contribute to demyelination in MS.

Mechanisms of ROS generation have been well-studied. The superoxide radical anion produced as a result of intrinsic inefficiencies in aerobic metabolism is relatively unreactive; however, it can be converted to the acutely reactive hydroxyl radical, which is capable of effecting indiscriminate damage to all biomolecules (Halliwell and Gutteridge, 2007). It has been shown that transition metals such as copper and iron are imperative for the production of hydroxyl radicals, and thus induction of biological damage (Fong, McCay, et al., 1973; McCord and Day, 1978). This metal-catalyzed conversion of superoxide radical to the hydroxyl radical has been dubbed the “metal-catalyzed Haber-Weiss reaction”, and occurs in two steps; the first being the reduction of the metal species by superoxide, and second, the reaction of the reduced metal with available hydrogen peroxide to produce a hydroxyl radical and re-oxidized metal, also known as the Fenton reaction. There is extensive literature implicating the hydroxyl radical as the ultimate cause of biological oxidative damage (Chevion, 1988; Shinar, Navok, and Chevion, 1983), especially by its ability to initiate lipid peroxidation (Fridovich and Porter, 1981) and cause irreversible protein modifications (Stadtman, 1990).

The extremely high reactivity of hydroxyl radicals means that they will attack target molecules within a few molecular encounters of their site of generation (Chevion, 1988). As transition metals are required for hydroxyl radical production, metal localization is inextricably linked to the site of their generation. Proteins may either contain a chelated transition metal prosthetic group, or have an inherent affinity for

redox-active metals such as iron and copper (Gutteridge and Halliwell, 1982). Thus, these binding sites become the sites at which hydroxyl radical-mediated damage is largely incurred. Binding of the metal to the biological target is necessary for the induction of damage, and removal of the metal from the biomolecule is sufficient for preventing this damage (Samuni, Aronovitch, et al., 1983; Shinar, Navok, and Chevion, 1983). Therefore, biological oxidative damage by hydroxyl radicals occurs in a site-specific fashion (Gutteridge and Wilkins, 1983).

In this study the effects of ROS and oxidative damage on myelin compaction were investigated. Myelin is a lipid-rich sheath that insulates axons of the peripheral nervous system (PNS) and the central nervous system (CNS), allowing for faster action potential propagation via saltatory conduction. Intersheet adhesion, and therefore compact structure, is predominantly mediated by Protein zero (P0) in the PNS and Proteolipid protein (PLP) in the CNS. In the PNS, homophilic interactions between P0 tetramers from opposing membranes are essential for both adequate myelination levels and the functionally critical step of myelin compaction (Shapiro, Doyle, et al., 1996). Thus, an intact P0 adhesive dimeric interface is integral to the development and function of PNS myelin.

The tight compaction of adjacent membranes of the myelin sheath is essential for its function, and disruption of this compaction by oxidative attack could compromise its electrical insulation properties (Bartzokis, 2004). The high lipid-to-protein ratio of myelin renders the tissue inherently vulnerable to oxidative damage (Smith, Kapoor, and Felts, 1999), as membrane lipids are able to sustain the propagative free radical chain

reaction known as lipid peroxidation, whereby initial formation of a lipid peroxy radical can abstract a hydrogen atom from an adjacent unsaturated fatty acid chain, forming a new lipid radical species that perpetuates the cycle (Gutteridge, 1995). It has been suggested that nerves in the PNS may be more sensitive to OS-induced demyelination than in the CNS given that markers of lipid peroxidation were elevated in PNS myelin only following oral administration of a copper accumulation-promoting compound to rats (Tonkin, Valentine, et al., 2004) despite the much larger body of work devoted to the effects of OS in the CNS. Additionally, levels of the important antioxidant, glutathione, are lower in the PNS than in the CNS (Romero, 1996). The studies herein will supplement what is known about the effects of OS on PNS myelin.

Myelin is unusually rich in the class of ether-linked phospholipids known as plasmalogens, with up to 70% of ethanamine glycerophospholipids existing as the plasmalogen form (Farooqui and Horrocks, 2001). Such an enrichment of plasmalogens has prompted investigations into their possible function. A potential role for plasmalogens as membrane-protecting antioxidants was first proposed twenty years ago, with the finding that plasmalogen-deficient mammalian cells were substantially more susceptible to OS-induced death than their plasmalogen-containing counterparts (Morand, Zoeller, and Raetz, 1988; Zoeller, Morand, and Raetz, 1988). Subsequent studies have suggested that plasmalogens interrupt the free radical chain reactions of lipid peroxidation, with the vinyl ether moiety preferentially attacked by oxygen radical species over the intrachain double bonds of unsaturated fatty acids (Reiss, Beyer, and Engelmann, 1997). However, reaction of the plasmalogen vinyl ether linkage with a

radical species, whether it be a hydroxyl radical or lipid peroxy radical, will inherently generate another radical species, thus provoking one to question how plasmalogens may suppress the process of lipid peroxidation. One proposed mechanism suggests that the vinyl ether radical species formed upon radical attack is less reactive than the allylic radical species formed after hydrogen abstraction adjacent to an intrachain double bond as occurred in standard polyunsaturated fatty chain (PUFA) chains (Sindelar, Guan, et al., 1999). This proposed lower reactivity would thus interfere with the propagation stage of lipid peroxidation. An alternative is that the position of the plasmalogen vinyl bond in close proximity to the polar head group region of a membrane bilayer reduces the likelihood that subsequent radical reactions will damage the polyunsaturated acyl chains located deeper within the membrane interior. In this scenario, the vinyl ether is preferentially attacked by ROS generated in the aqueous phase and therefore closer to lipid polar head groups, saving intrachain double bonds from such damaging reactions (Engelmann, 2004; Morandat, Bortolato, et al., 2003; Murphy, 2001). Though the biochemical mechanism by which plasmalogens preserve membrane integrity and cell viability against oxidative insult remains under investigation, a wide range of studies have implicated a role of plasmalogens as endogenous membrane antioxidants. The generation of plasmalogen-deficient mouse strains (Brites, Motley, et al., 2003) has facilitated the investigation of potential plasmalogen antioxidant capacity in myelin. Demonstration of a protective effect would provide an explanation for the particular enrichment of plasmalogen lipids in myelin.

Given that myelin compaction is imperative for function, it will be crucial to examine ROS-mediated structural changes. X-ray diffraction is a valuable tool for the high-resolution determination of internodal myelin membrane structure in intact, unfixed nerves (Caspar and Kirschner, 1971). The use of x-ray diffraction to characterize membrane structure affords rapid quantitative results and avoids the lengthy tissue processing time and potential artifacts associated with EM. Data obtained from myelin diffraction can be used to calculate the repeat period of myelin arrays, protein and lipid localization within arrays, and the relative amount of myelin in whole nerves. Here it will be used to examine the *ex vivo* effects of ROS on myelin compaction.

Earlier work has shown that isolated CNS myelin undergoes decompaction upon exposure to a copper and hydrogen peroxide ROS-generating system (Bongarzone, Pasquini, and Soto, 1995). However, it is possible that isolated myelin obtained from homogenized nerves may be differentially susceptible to ROS than myelin on intact nerves. More recently, a link between dithiocarbamate-mediated copper accumulation, lipid peroxidation, and myelin structural lesions has been demonstrated *in vivo* in rat peripheral nerve (Viquez, Valentine, et al., 2008). However, the mechanism by which copper contributes to myelin structural abnormalities was not provided, which we investigate in the current study.

In order to examine whether plasmalogen phospholipids protect myelin sheaths from oxidative damage, a ROS-generating system that reproducibly induced changes to *ex vivo* myelin compaction was first developed. The ability of the copper-hydrogen peroxide system to generate hydroxyl radicals is well-characterized (Chevion, 1988) and

biologically relevant and was thus utilized here. As hydroxyl radicals are generated at sites of copper itself, we also added the lipophilic copper chelator, o-phenanthroline (OP), which enables the transport of copper through membranes (Goldstein and Czapski, 1986). As myelin is particularly enriched in lipid components compared with other membranes, the addition of a lipophilic chelator was imperative for the induction of irreversible structural changes associated with oxidative damage. In the current work, we show that copper must be localized on or within myelin membrane bilayers in order to cause irreversible myelin decompaction in both optic and sciatic nerves, and that a hydroxyl radical-dependent mechanism is likely. Most intriguingly, we found that sciatic nerve myelin from plasmalogen-deficient mice was significantly more susceptible to ROS-mediated decompaction than that from WT mice, implicating plasmalogen phospholipids as endogenous antioxidants that play a role in preserving myelin structure in the presence of oxidative stress.



## **Materials and Methods**

### *Mice*

Mice used were kindly provided by Dr. Tom Seyfried (Boston College Biology Department, DDY WT inbred strain) or by Dr. Pedro Brites for use in collaborative efforts (Pex7 KO and WT littermates as described (Brites, Motley, et al, 2003)). Animals were housed in the Boston College Animal Facility and cared for according to IACUP protocol guidelines. Animals were sacrificed by cervical dissociation before dissection of sciatic nerves.

### *Nerve incubation/ ROS-generating system*

Sciatic nerves were dissected from freshly sacrificed animals, and the tissue was continuously rinsed with phosphate-buffered saline (PBS, 154 mM NaCl, 5 mM sodium phosphate pH 7.4) to ensure nerve structural integrity. Sciatic nerves were cut along their length to generate three different segments per nerve and thus allow conduction of three separate incubation experiments. Nerves were tied at the ends with silk suture thread (Harvard Apparatus, Holliston, MA) to facilitate the subsequent incubation and x-ray diffraction process. Nerve segments were gently stretched by securing attached suture threads to the ends of a plastic pipet tip before incubation in 20 mL PBS (154 mM NaCl and 20 mM sodium phosphate buffer pH 8.0; NaCl, sodium phosphate monobasic and dibasic from Sigma-Aldrich Inc.) with the indicated ROS-generating system components (CuSO<sub>4</sub>, *o*-phenanthroline, hydrogen peroxide 35 wt. % in H<sub>2</sub>O, formic acid, ethylenediaminetetraacetic acid disodium salt dehydrate 98%, all obtained from Sigma-Aldrich Inc.) for 72 hours (sciatic nerves) or 24 hours (optic nerves) at RT with gentle

rotary shaking (< 80 rpm). Following incubation, nerves were removed from the solution and loaded into 0.7 mm quartz capillaries (Charles Supper Co., Natick, MA) filled with the same solution. Ends were sealed with wax to prevent fluid evaporation and to allow gentle stretching of nerve, ensuring parallel nerve fiber alignment during diffraction.

For fixation, PBS or Cu/OP/HP-treated nerves were incubated in 2% glutaraldehyde (8% solution in water, Sigma-Aldrich Inc.) and 0.12 M sodium phosphate pH 7.4 (Sigma-Aldrich Inc.) for 5 days before XRD and/or further processing for EM.

#### *X-ray diffraction and myelin structure analysis*

Diffraction experiments were carried out using CuK $\alpha$  fine-line radiation from a Rigaku x-ray generator (Rigaku/MSI Inc., the Woodlands TX 77381-5209) operated at 40 kV by 14 mA, and diffraction patterns were recorded with a linear, position-sensitive detector (Molecular Metrology Inc, Northampton, MA 01060). Calibration by the determination of specimen-to-film distance (SFD; nomenclature reflects historical use of X-ray film rather than detector) was established by patterns from a sodium behenate powder standard, which has a fundamental spacing of  $d_{001} = 58.38 \text{ \AA}$ . Patterns were fit with Gaussian curves to allow precise determination of the centers of the diffraction peaks, and the SFD was derived using Bragg's law ( $n\lambda = 2d\sin\theta$ ;  $n$  = Bragg order,  $\lambda = 1.542 \text{ \AA}$ ,  $d = n * 58.38 \text{ \AA}$ ,  $2\theta$  = angle from center of beam to  $n$ th Bragg order peak) and by solving for SFD in  $\tan 2\theta = \text{channel coordinate of } n\text{th Bragg peak}/\text{SFD}$ . The SFD was expressed in the units of channel number, and ranged from 7997 to 8011 throughout all experiments discussed herein.

Measurements of myelin structure conducted by aligning the nerve perpendicular to incident beam, which was 200  $\mu\text{m}$  x 3 mm in size at the sample location, and thus with nerve fibers and beam in the same plane. Diffraction patterns were obtained following a 30 minute exposure time and analyzed with PeakFit software (Jandel Scientific, Inc.). Background x-ray scatter was defined as that below a line drawn connecting the local intensity minima, and subtracted from the overall scatter. Diffraction peaks were fit with Gaussian distributions for the determination of peak center and area. The repeat period of the myelin arrays was calculated by Bragg's law, using the channel number of all peak centers corresponding to the observed Bragg orders. Depending on mouse genotype, the sciatic nerve myelin repeat period ranged from 174 to 177  $\text{\AA}$ . If multiple arrays were detected within a given pattern, repeat periods were calculated for each from the corresponding diffraction peaks. The relative amount of myelin ( $M/(M+B)$ ) of each nerve sample was calculated by dividing the sum of all peak areas (M) by the total scatter intensity (M+B), following subtraction of scatter due to the beam itself ( $\pm 50$  channels from beam center). The % of scatter from native myelin arrays (N/M) was calculated by dividing the sum of peak areas corresponding to native myelin arrays (N) by the sum of all myelin-derived peaks (M). "Native" myelin arrays were defined as those having a repeat period between 168 and 180  $\text{\AA}$ .

## Results

### *Sciatic nerve myelin undergoes decompaction after exposure to a membrane-targeted hydroxyl radical-generating system*

Our first aim was to develop an in vitro ROS-generating system that induces oxidative structural alterations to myelin. The ability of the Cu/HP system to induce oxidative modification to biological molecules via site-specific hydroxyl radical production is well-characterized (Fig. 1) (Chevion, 1988). We thus incubated freshly dissected intact DDY sciatic nerve segments for 72 hr with Cu (100  $\mu$ M), HP (20 mM), or both, before collecting x-ray diffraction data for 30 min. Sciatic nerve myelin retained native 176 Å periodicity when incubated in 100  $\mu$ M Cu or 20 mM HP alone as expected, given that these conditions are not reported to cause oxidative damage to biomolecules (Chan, Peller, and Kesner, 1982; Samuni, Aronovitch, et al., 1983). In the presence of both Cu and HP, the reaction between which produces damaging hydroxyl radicals, myelin also retained native periodicity. However, upon co-incubation with 100  $\mu$ M of the lipophilic copper chelator o-phenanthroline (OP), Cu, and 20 mM HP, myelin underwent dramatic structural changes corresponding to decompaction of both the cytoplasmic and extracellular appositions resulting in >210 Å periodicity (Fig. 2A). XRD scatter from myelin arrays in their native, compacted, state was significantly reduced (Fig. 2B). Myelin decompaction was likely caused by the ability of OP to enable transport of Cu through the myelin membranes (Goldstein and Czapski, 1986), thereby facilitating

reaction between Cu and HP within the membrane bilayers. This would cause the generation of membrane-targeted hydroxyl radicals, damaging myelin proteins and lipids that are essential for preserving membrane compaction. Cu/HP treatment alone was therefore unlikely to generate radical species within the immediate proximity of myelin membranes. When Cu/OP/HP-treated nerves were re-incubated in PBS for nine hrs, membranes remained in their decompacted state, indicating the induction of irreversible Cu/OP/HP-mediated damage (Fig. 2A). In contrast, membrane decompaction observed upon incubation in low pH conditions can be reversed by subsequent incubation in PBS at pH 7.4 (Avila 2007). Incubation of sciatic nerves in Cu and OP alone induced neither decompaction nor other structural defects (Fig. 2), demonstrating that localization of the metal to the membrane interior alone was not sufficient to cause decompaction.

In order to further examine the effects of Cu/OP/HP treatment on myelin structure, DDY mouse sciatic nerve segments were incubated in PBS alone or in Cu/OP/HP for 72 h at RT. Nerves were then fixed in 2% glutaraldehyde/0.12 M phosphate buffer, which was previously determined to be an optimal fixative for preserving the structural integrity of myelin membranes (Avila 2007). X-ray diffraction patterns of the fixed, PBS or Cu/OP/HP pre-treated nerves were then obtained to determine whether the process of fixation itself had caused alterations in myelin structure (Fig. 3). Fixation did cause moderate decompaction in PBS-alone treated nerves ( $d = 193 \text{ \AA}$  after fixation, compared with  $d = 177 \text{ \AA}$  before), but had very little effect on the Cu/OP/HP-treated nerves ( $d = 227 \text{ \AA}$  after fixation, compared with  $d = 224 \text{ \AA}$  before). These same nerves were then sent for electron microscopy (EM) processing examination. It is evident from EM that

Cu/OP/HP-treatment causes myelin membrane decompaction and disordering (Fig. 4). Thus, both XRD and EM demonstrate that the ROS-generating system used here causes gross structural alterations in myelin structure.

Additional experiments were then conducted to validate the direct role of reactive oxygen species in Cu/OP/HP-mediated myelin decompaction. Sodium formate (formate) is an established hydroxyl radical scavenger that has been used extensively to implicate these species in effecting biological damage (Chan, Peller, and Kesner, 1982; Chevion, 1988; Que, Downey, and So, 1980). Addition of formate (10 and 20 mM) to Cu/OP/HP-incubated sciatic nerves prevented decompaction in a dose-dependent manner, as can be seen by the presence of diffraction peaks corresponding to those of the PBS-treated control (Fig. 5A) and quantified in Fig. 5B. Formate-mediated prevention of Cu/OP/HP-induced decompaction was highly significant (Figure 4,  $p = 0.009$ , Cu/OP/HP vs. Cu/OP/HP/20 mM form).

As copper chelation by OP was found to be imperative for ROS-mediated myelin decompaction, it was reasoned that a water-soluble Cu-chelator may be able to prevent this decompaction. EDTA can successfully compete with OP for Cu binding (Gutteridge and Halliwell, 1982), thus sequestering Cu in the bulk incubation solution and away from the myelin membrane target (Chevion 1988). The addition of EDTA prevented Cu/OP/HP-induced decompaction, with the percentage of x-ray scatter from native myelin arrays statistically indistinguishable from that of the PBS control (Fig. 6).

Taken together, these results provide evidence for a Cu/OP/HP-mediated production of hydroxyl radicals within, and damage to, the myelin membranes, leading to

an irreversible decompaction. Sequestration of Cu by EDTA, presumably within the bulk solution away from the membrane targets, was sufficient to prevent Cu/OP/HP-mediated damage.

*Plasmalogen phospholipids offer sciatic nerve myelin protection from ROS-mediated decompaction*

Plasmalogen phospholipids have been implicated as endogenous protectors against oxidative insults (Morand, Zoeller, and Raetz, 1988; Zoeller, Morand, and Raetz, 1988), and are particularly enriched in myelin membranes (Farooqui and Horrocks, 2001), suggesting a role in potential protection from the highly oxidative environment in neuronal tissue. Pex7 KO mice have dramatically reduced levels of plasmalogen phospholipids in all tissues due to impaired peroxisomal import of an essential plasmalogen biosynthesis enzyme (Brites, Motley, et al, 2003), and thus in comparison with WT littermates, can be used to examine whether plasmalogens may have a protective role against oxidative insult to myelin membranes.

In order to determine whether there exist any myelin structural abnormalities or packing instability associated with plasmalogen deficiency that could confound studies of ROS susceptibility, sciatic nerves from Pex7 KO and WT littermates were dissected and incubated for 72 hr at RT in PBS before examination with XRD. Myelin periodicity was not significantly different from WT ( $p = 0.22$ ), indicating that plasmalogen deficiency does not compromise myelin packing stability (Fig. 7). The relative amount of myelin of

Pex7 KO nerves was slightly lower than of WT nerves (Fig. 7,  $p = 0.045$ ), as was the % of this myelin found in native, compacted arrays (Fig. 9, PBS). However, these differences were small, and more importantly the myelin repeat period was not statistically different, thus allowing the examination of ROS-mediated effects on compaction without prohibitory confounding variables. These findings indicate that sciatic nerve myelin from Pex7 KO animals possesses similar structural stability as that from WT animals.

We then examined Cu/OP/HP dose-dependent decompaction of WT sciatic nerve myelin; this was conducted to find intermediate concentrations of ROS-generating components that may differentially affect WT and Pex7 KO myelin. After 72 hrs incubation in 5 mM HP in the presence of Cu/OP (100 $\mu$ M/100  $\mu$ M), WT sciatic nerve myelin largely maintained its native, 174 Å-compacted state as evidenced by the percentage of total x-ray scatter emanating from compact myelin arrays (Fig. 8,9 WT). After incubation in Cu/OP/10 mM HP, WT sciatic nerve myelin still largely retained its native compaction; only the highest dose of 20 mM HP induced near total decompaction (Fig. 8,9 WT).

Having shown that WT sciatic nerve myelin undergoes decompaction in a Cu/OP/HP dose-dependent fashion, we then evaluated the susceptibility of Pex7 KO sciatic nerve myelin to these conditions. In contrast to WT, a substantial proportion of Pex7 KO myelin underwent decompaction after incubation in Cu/OP/5 mM HP, with the XRD scatter from native compact myelin comprising less than 50% of total myelin scatter in 3 separate experiments (Fig. 8A, Fig. 9). At the higher 10 mM HP dose, scatter



from native, compacted myelin was almost undetectable; nearly all membrane arrays were found to have decompacted to  $>210\text{\AA}$  periodicity (Fig. 8B, Fig. 9). In contrast, 80% of sciatic nerve myelin from WT animals remained in its native compacted state after identical Cu/OP/10 mM HP treatment (Fig. 8B, Fig. 9). These findings were highly statistically significant with  $p < 0.0001$ . Thus, these results indicate that plasmalogen-deficient myelin has a heightened sensitivity to ROS-mediated decompaction.

It was found that the radical scavenger sodium formate was able to partially protect WT sciatic nerve myelin from Cu/OP/HP-induced decompaction, implicating the central role of hydroxyl radicals in this effect. Therefore, formate should similarly be capable of protecting Pex7 KO myelin from the effects of the Cu/OP/HP ROS-generating system; this protection would demonstrate that a ROS-scavenging defect in Pex7 KO myelin is resulting in the heightened sensitivity to Cu/OP/HP. The lowest concentration of HP that in the presence of Cu/OP caused complete decompaction in WT and Pex7 KO animals was used to determine whether formate could offer protection. It was found that formate was able to partially prevent Cu/OP/HP-mediated decompaction of Pex7 KO nerves, though 20 mM formate was not as effective at preserving native membrane structure as in WT nerves (Fig. 10, 11). Though two different experiments were shown, more data would be needed to demonstrate that formate statistically prevents decompaction in Pex7 KO sciatic nerve myelin.

Together, these results demonstrate that myelin from Pex7 KO sciatic nerves is more sensitive to ROS-induced decompaction, implicating plasmalogen phospholipids as

endogenous antioxidants capable of preserving native myelin compaction after exposure to an oxidative insult.

#### *Effects of ROS on optic nerve myelin decompaction*

Optic nerve myelin also underwent irreversible decompaction upon exposure to the Cu/OP/HP ROS-generating system, and similarly maintained predominantly native periodicity when incubated in either Cu or HP alone (Fig. 12). Myelin periodicity increased dramatically from 157 Å to >230 Å after 24 hours in the present of Cu/OP/HP. Nerve incubation time was reduced to 24 hours, versus 72 hours in sciatic nerve, as longer incubation in Cu/OP/HP was found to compromise whole nerve structural integrity that prevented capillary loading of the nerve. Optic nerves are not protected by connective tissue to the same extent as are sciatic nerves, and thus ROS treatment may more rapidly cause nerve damage. The effects of Cu/OP/HP on optic nerve myelin structure were confounded by the ability of HP and Cu/OP alone to induce decompaction; this was in disagreement with findings from sciatic nerve studies and known requirements for ROS-mediated damage. Optic nerve myelin may be intrinsically more sensitive to these incubation components, and the concentration of ROS-generating components may need adjustment such that severe structural changes are not observed in the absence of requisite ROS generation components. A mechanism for the differential optic nerve ROS susceptibility observed here would contribute to the general understanding of what mediates ROS-dependent decompaction.

Characterization of the effects of ROS on Pex7 KO optic nerve myelin decompaction was precluded by the number of animals available and the small size of the nerves, which prevented segmenting as with sciatic nerves that allowed for three diffraction experiments per nerve. Furthermore, Pex7 KO optic nerves are severely hypomyelinated (Avila 2007), which would confound studies of ROS-susceptibility.

## Discussion

We have demonstrated that *ex vivo* exposure of sciatic and optic nerves to an ROS-generating system causes irreversible membrane decompaction, and that sciatic nerve myelin from plasmalogen-deficient mice possesses a heightened sensitivity to decompaction caused by the oxidative insult. The decompaction caused by exposure to the Cu/OP/HP system is presumably mediated by hydroxyl radicals, as evidenced by the protective effect of the well-known hydroxyl radical scavenger, sodium formate. Given that plasmalogen phospholipids also protected myelin membranes from ultrastructural damage induced by Cu/OP/HP incubation, evidence for the role of plasmalogens as ROS scavengers has been provided. Such a role may explain their particular enrichment in myelin membranes.

We found that hydroxyl radical production must be targeted to the myelin membranes via the lipophilic copper chelator OP in order to cause decompaction; hydroxyl radicals produced in the bulk incubation solution by Cu-EDTA sequestration did not induce changes in myelin structure (Fig. 6). This finding is in accord with the site-specific model of transition metal-catalyzed oxidative damage, whereby hydroxyl radicals inflict damage at the site of their formation – at the metal binding site – because of their extremely high reactivity (Chevion, 1988). The site-specific mechanism of damage may be particularly true in the case of membranes, as hydroxyl radicals generated in aqueous surroundings would have little chance of initiating lipid peroxidation in the membrane interior (Schaich, 1992). Thus, the known ability of OP to enable transmembrane Cu transport (Goldstein, and Czapski, 1986; Samuni, Aronovitch,

et al., 1983) was required to induce myelin ultrastructural damage as demonstrated here. This is also supported by the protective effect of EDTA (Fig. 6), which can compete with OP for Cu binding and sequester the metal in the bulk incubation solution (Gutteridge and Halliwell, 1982). It is not known whether OP chelation causes Cu to localize within the bilayer interior or within the polar head group region.

Formate was found to mitigate membrane damage induced by Cu/OP/HP exposure; however, the concentrations used here were likely not high enough to completely protect against oxidative decompaction. Higher concentrations were not utilized as myelin can undergo decompaction simply by incubation in a high ionic strength solution (Inouye, and Kirschner, 1988), which would have confounded the detection of a greater protective effect against the ROS insult. The incomplete protection afforded by formate is in agreement with prior studies on ROS damage to biomolecules, and can be explained by the site-specific theory of transition metal-catalyzed free radical damage. It has been reported that scavenger concentrations as high as 0.1 to 1 M are required to ensure that sufficient amounts are present at the site of radical generation and can therefore effectively scavenge nascent hydroxyl radicals (Goldstein and Czapski 1986).

The biochemical mechanism by which Cu/OP/HP treatment causes myelin membrane decompaction remains to be elucidated. Homodimeric interactions of the major myelin adhesive protein, P0, are requisite for proper compaction (Shapiro, Doyle, et al., 1996), and thus it is reasonable to speculate that Cu/OP/HP may induce oxidative modifications to P0 that disrupt the contact interfaces given the damaging effects of ROS

on myelin proteins that have been demonstrated in investigations using isolated CNS myelin (Konat and Wiggins, 1985). One must also consider the potential roles of lipid peroxidation in mediating decompaction, given that OP can transport Cu through, and potentially localize to, the membrane interior. The role of lipid peroxidation in potentially mediating myelin decompaction becomes especially important when considering the observed protective effect of plasmalogen phospholipids.

Though the chemical mechanism by which Cu/OP/HP causes myelin damage has not been experimentally determined, our results show that plasmalogen phospholipids are capable of protecting against this ultrastructural damage by comparison of WT and Pex7 KO myelin ROS-susceptibility. Many prior studies have investigated the ability of plasmalogens to mitigate PUFA peroxidation in model membrane systems (Reiss, Beyer, and Engelmann, 1997); however, several different mechanisms accounting for the antioxidant effect have been proposed. The prevailing notion seems to be that plasmalogens interfere with the propagation, rather than initiation, step of lipid peroxidation (Morandat, Bortolato, et al., 2003; Murphy, 2001). Thus, peroxidation of a PUFA by a hydroxyl radical first generates a lipid peroxy or alkoxy radical (initiation), which then reacts with plasmalogen vinyl ether, forming a new vinyl ether radical species (Sindelar, Guan, et al., 1999). How would the formation of a new radical species constitute a protective antioxidant mechanism? Two theories have been proposed to account for this apparent paradox. First is that the radical species formed from vinyl ether oxidation is more chemically stable than the alkoxy radical that would be generated after transition-metal catalyzed lipid hydroperoxide degradation and thus unable to

initiate PUFA peroxidation (Sindelar, Guan, et al., 1999). A second possibility takes into account the proximity of the vinyl ether moiety to the polar head group region of membrane bilayers (Murphy, 2001). The 1'C carbon vinyl ether radical formed following ROS radical attack is sterically segregated from the bulk pool of polyunsaturated fatty acids in the membrane interior, and potentially is unable to propagate further radical reactions given the lack of susceptible C-H bonds (Murphy, 2001). Plasmalogen-deficient sciatic nerve myelin was significantly more susceptible to ROS-mediated decompaction than was WT myelin, but this susceptibility to decompaction was restored to near WT levels when co-incubated with sodium formate. This raises the possibility that formate is serving a similar role as plasmalogen in protecting against Cu/OP/HP-mediated decompaction. Formate is an anionic, water-soluble compound, and may not be able to penetrate deep within the bilayers. If the Cu-OP complex, which serves as the nucleation site for hydroxyl radical production, similarly localizes near the polar head group region of the bilayer, then formate would have the opportunity to scavenge the hydroxyl radicals formed upon Cu-OP reaction with HP (Schaich, 1992). Similarly, the vinyl ether moiety of the plasmalogen lipids resides by the polar head group region and potentially could react with locally produced hydroxyl radicals, preventing their reaction with PUFAs and initiation of lipid peroxidation in the membrane interior.

The precise mechanism of plasmalogen ROS scavenging remains to be determined, both in light of the current findings and in general. Analysis of PUFA degradation following Cu/OP/HP treatment of WT and Pex7 KO nerves would indicate whether plasmalogen phospholipids can protect from this effect. It could also be

examined whether plasmalogens protect myelin proteins from damage upon ROS exposure by Western blotting and/or mass spectroscopy of whole nerve homogenate.

In summary, an ROS-generating system capable of causing *ex vivo* sciatic and optic nerve myelin decompaction has been developed. The decompaction was found to be dependent on membrane-targeted hydroxyl radical production, as evidenced by the protective roles of a hydroxyl radical scavenger and the water-soluble cation chelator EDTA. The enhanced susceptibility of sciatic nerve myelin from plasmalogen-deficient mice to decompaction upon ROS exposure suggests that these lipid species may play a role as endogenous antioxidants in myelin. Plasmalogens *in vivo* may therefore play an important role in the preservation of myelin structural integrity during aging- and neurodegenerative disease-associated oxidative stress.



## Figures

**Figure 1.** Mechanism of *in vitro* ROS production.

- A. Cu (II) is reduced by hydrogen peroxide (HP) to produce Cu(I) and a hydroperoxyl radical, which rapidly deprotonates to form the largely unreactive superoxide radical. The reduced Cu(I) species reacts with another equivalent of HP to generate a hydroxyl radical, regenerating Cu(II). This cycle will proceed until HP is quenched. Arrows indicate components added during *in vitro* ROS production.
- B. Schematic showing that the site of hydroxyl radical damage is dependent on the site of metal (copper in this case) localization.

**Figure 1.** Mechanism of *in vitro* ROS production.

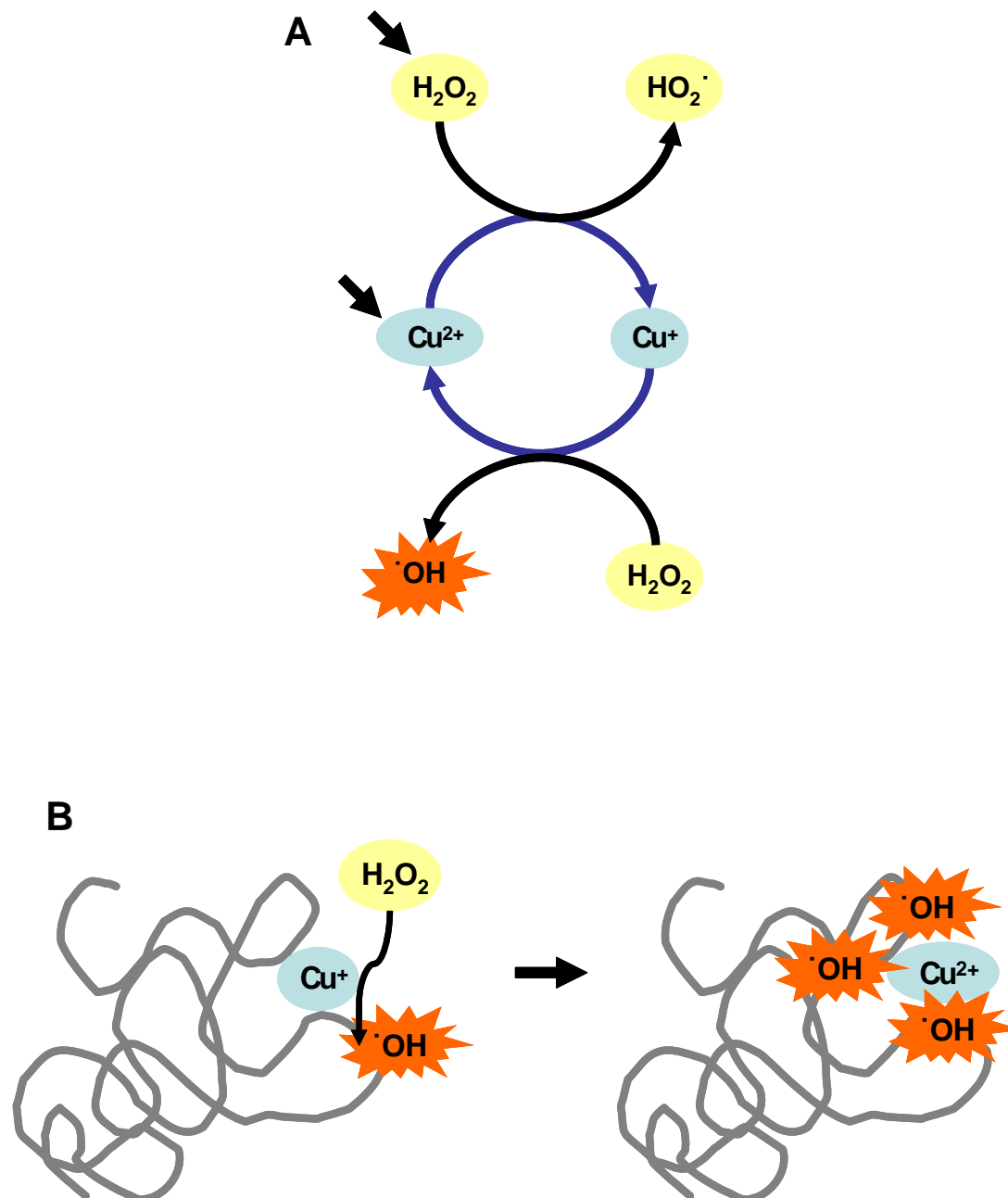


**Figure 2.** Incubation of sciatic nerves with an ROS-generating system induces irreversible myelin decompaction.

A. Representative XRD patterns from DDY mouse sciatic nerves incubated 72 h at RT in Cu (100  $\mu$ M), OP (100  $\mu$ M), and/or HP (20 mM) as described in materials and methods.

A Cu/OP/HP-treated nerve was additionally incubated in PBS for 24 hr before x-ray diffraction. Patterns are shown vertically displaced from each other for enhanced clarity.

B. Quantification of x-ray scatter from myelin arrays in native, compacted state from DDY mouse sciatic nerves incubated as in A. The total scatter attributed to native myelin arrays was divided by the total scatter after background subtraction. The averages and standard deviations were calculated from eleven (PBS), three (Cu), five (Cu/OP), one (HP), two (Cu/HP) and thirteen (Cu/OP/HP) separate experiments.

**Figure 2.** Incubation of sciatic nerves with an ROS-generating system induces irreversible myelin decompaction.

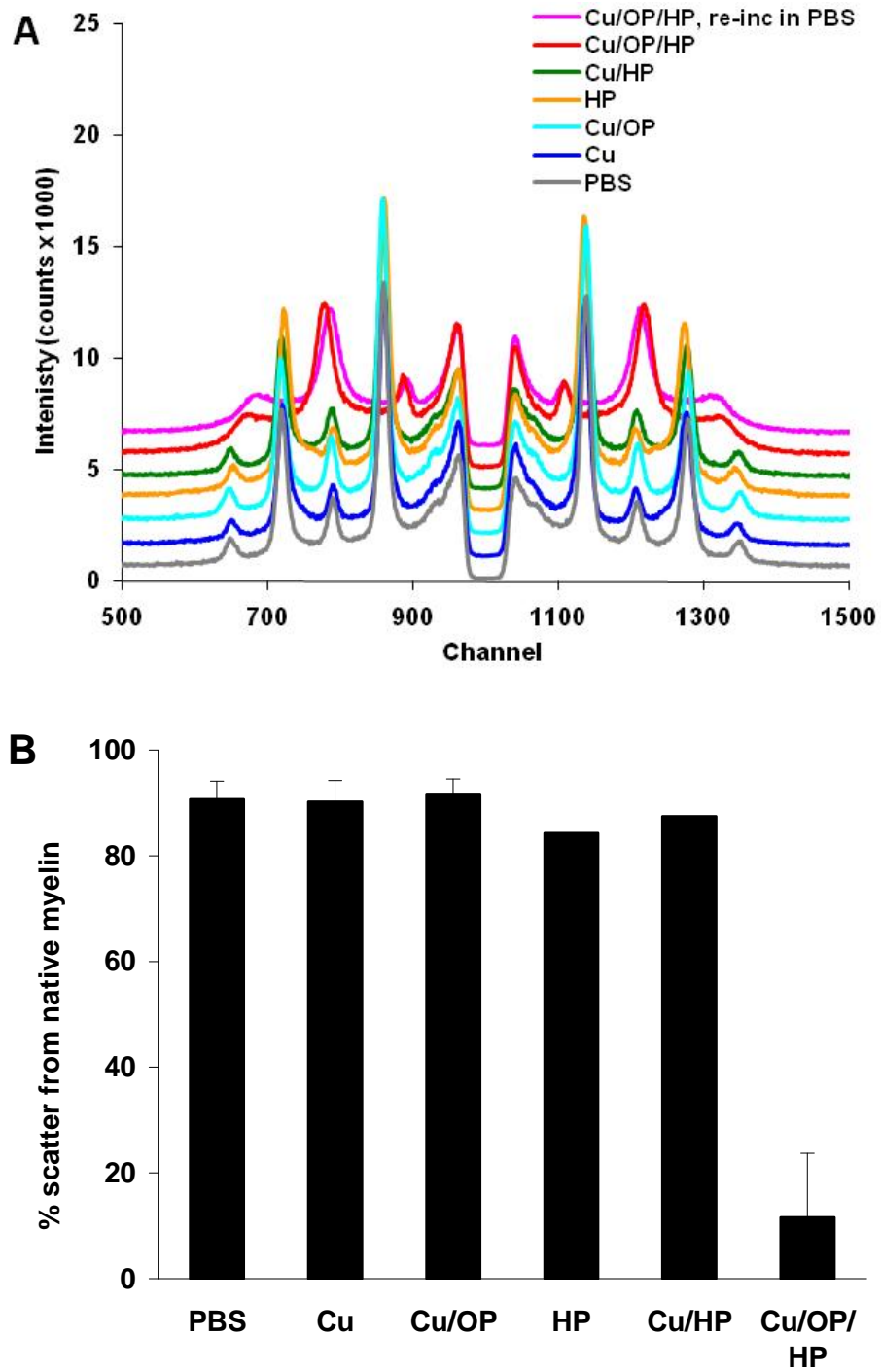


**Figure 3.** Glutaraldehyde fixation does not change myelin packing of control or Cu/OP/HP-treated sciatic nerves.

A. XRD patterns from DDY mouse sciatic nerves incubated 72 h at RT in PBS and either analyzed immediately (PBS fresh) or fixed at RT for five days in 2% glutaraldehyde/0.12 M sodium phosphate pH 7.4 (PBS fixed). Nerves were mounted in 0.7 mm quartz capillaries filled with their respective incubation solution before obtaining diffraction patterns for 30 min. Patterns are shown vertically displaced from each other for enhanced clarity.

B. XRD patterns from DDY mouse sciatic nerves incubated 72 h at RT in PBS + Cu (100  $\mu$ M), OP (100  $\mu$ M), and/or HP (20 mM) and either analyzed immediately (Cu/OP/HP fresh) or fixed at RT for five days in 2% glutaraldehyde/0.12 M sodium phosphate pH 7.4 (Cu/OP/HP fixed). Nerves were mounted in 0.7 mm quartz capillaries filled with their respective incubation solution before obtaining diffraction patterns for 30 min.

**Figure 3.** Glutaraldehyde fixation does not change myelin packing of control or Cu/OP/HP-treated sciatic nerves.

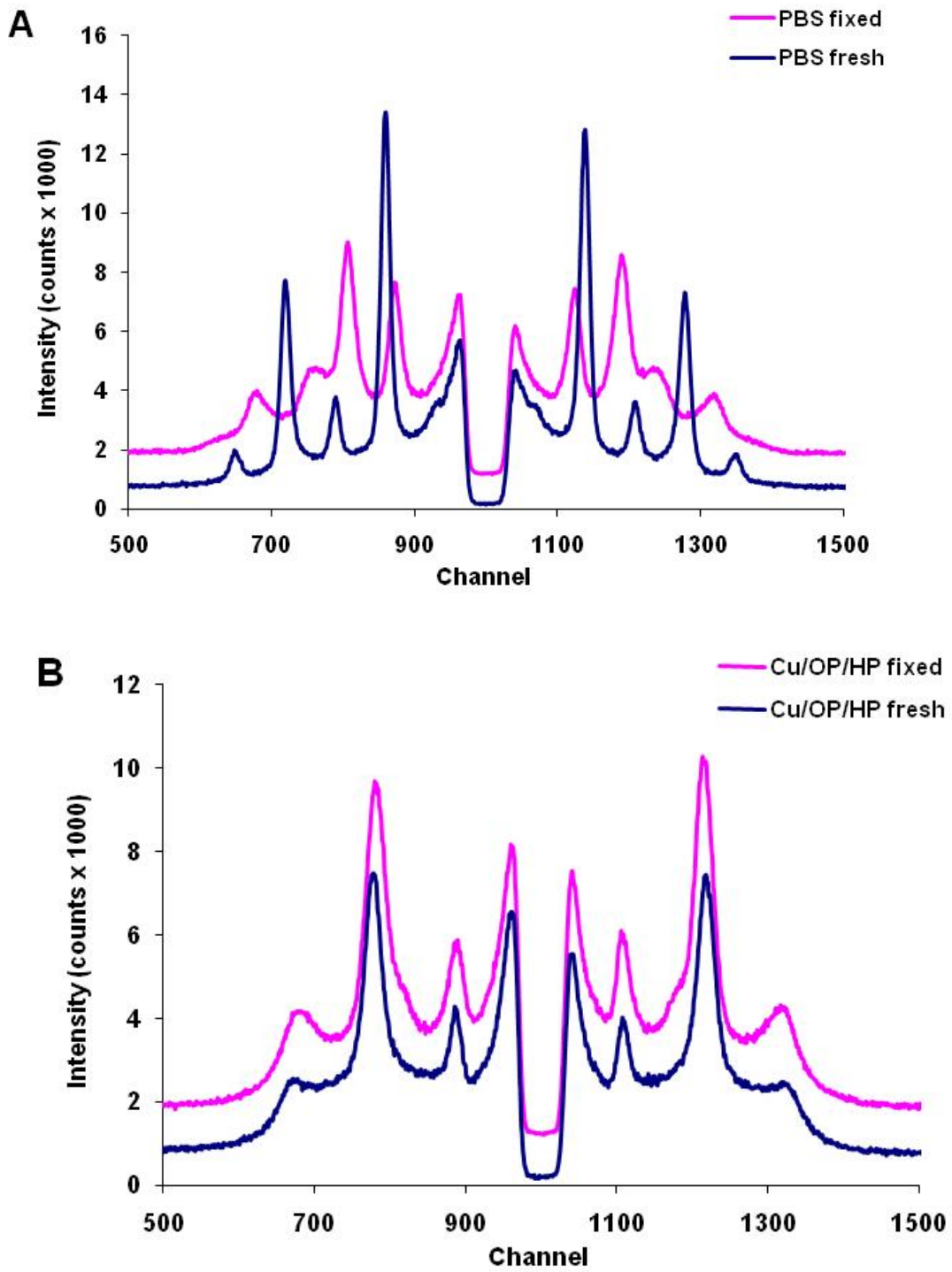


**Figure 4.** Cu/OP/HP sciatic nerve treatment causes disordering and decompaction of myelin lamellae.

Sciatic nerves from DDY mice were incubated with PBS or with HP/Cu/OP as described in Figure 1a, and then fixed for five days in 2% glutaraldehyde/0.12 M sodium phosphate pH 7.4. EM images were obtained following OsO<sub>4</sub> staining, dehydration, embedding, and thin sectioning.

A. EM of sciatic nerve myelin that had been incubated for 72 h at RT in PBS before fixation and processing.

B. EM of sciatic nerve myelin that had been incubated for 72 h at RT in Cu (100 μM), OP (100 μM), and HP (20 mM) before fixation and processing.

**Figure 4.** Cu/OP/HP sciatic nerve treatment causes disordering and decompaction of myelin lamellae.

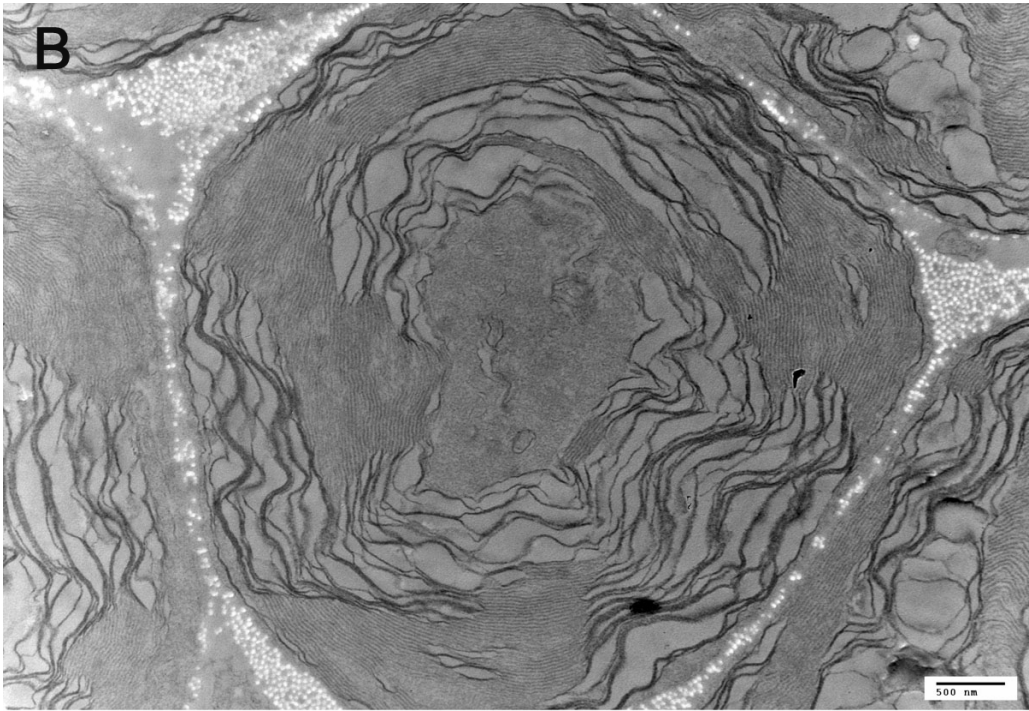
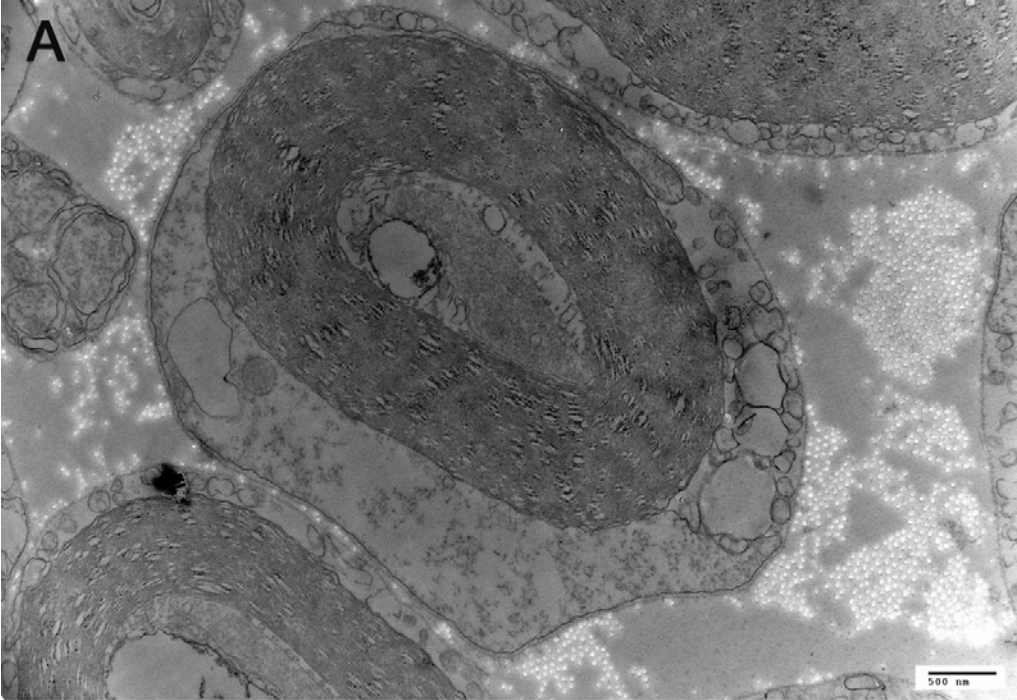




**Figure 5.** Cu/OP/HP-induced sciatic nerve myelin decompaction is mitigated by addition of a hydroxyl radical scavenger.

A. Representative XRD patterns from DDY mouse sciatic nerves incubated 72 h at RT in PBS alone, Cu (100  $\mu$ M), OP (100  $\mu$ M), and HP (20 mM), or Cu/OP/HP with sodium formate (10 or 20 mM). Patterns are shown vertically displaced from each other for enhanced clarity.

B. Quantification of x-ray scatter from myelin arrays in native, compacted state after treatment as in A. The total scatter attributed to native myelin arrays was divided by the total scatter after background subtraction. The averages and standard deviations were calculated from eleven (PBS), thirteen (Cu/OP/HP), two (Cu/OP/HP/10 mM form) and four (Cu/OP/HP/20 mM form) separate experiments. \*\*  $p = 0.009$ , Cu/OP/HP vs. Cu/OP/HP 20 mM form.

**Figure 5.** Cu/OP/HP-induced sciatic nerve myelin decompaction is mitigated by addition of a hydroxyl radical scavenger.

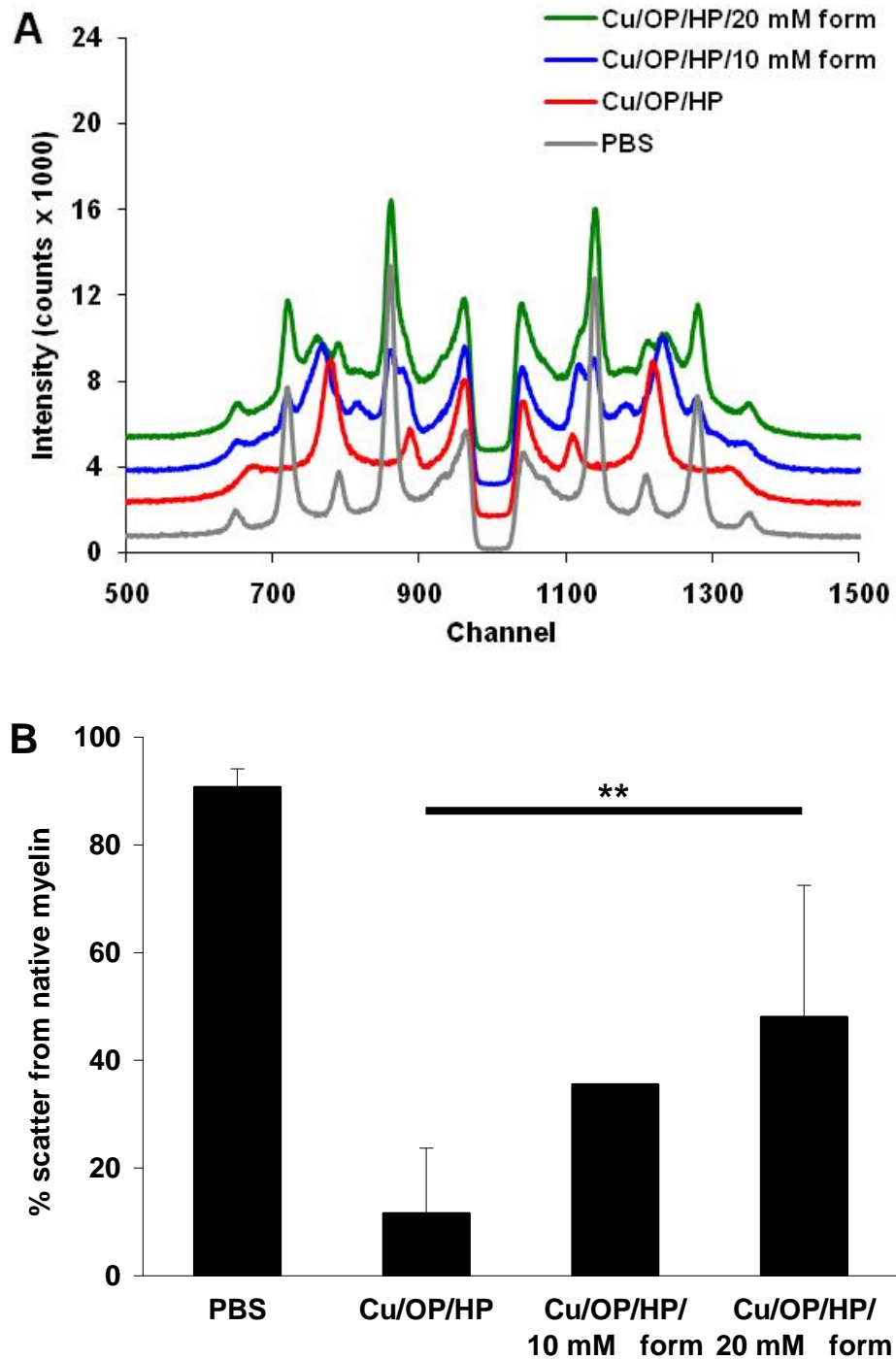


**Figure 6.** EDTA largely prevents Cu/OP/HP-mediated sciatic nerve myelin decompaction.

(a) Representative XRD patterns from DDY mouse sciatic nerves incubated 72 h at RT in PBS alone, Cu (100  $\mu$ M), OP (100  $\mu$ M), and HP (20 mM), or Cu/OP/HP with EDTA (1 mM). Patterns are shown vertically displaced from each other for enhanced clarity.

(b) Quantification of x-ray scatter from myelin arrays in native, compacted state. The total scatter attributed to native myelin arrays was divided into the total scatter after background subtraction. The averages and standard deviations were calculated from eleven (PBS), thirteen (Cu/OP/HP), and three (Cu/OP/HP/EDTA) separate experiments.

\*\*  $p = 0.0002$ .

**Figure 6.** EDTA largely prevents Cu/OP/HP-mediated sciatic nerve myelin decompaction.

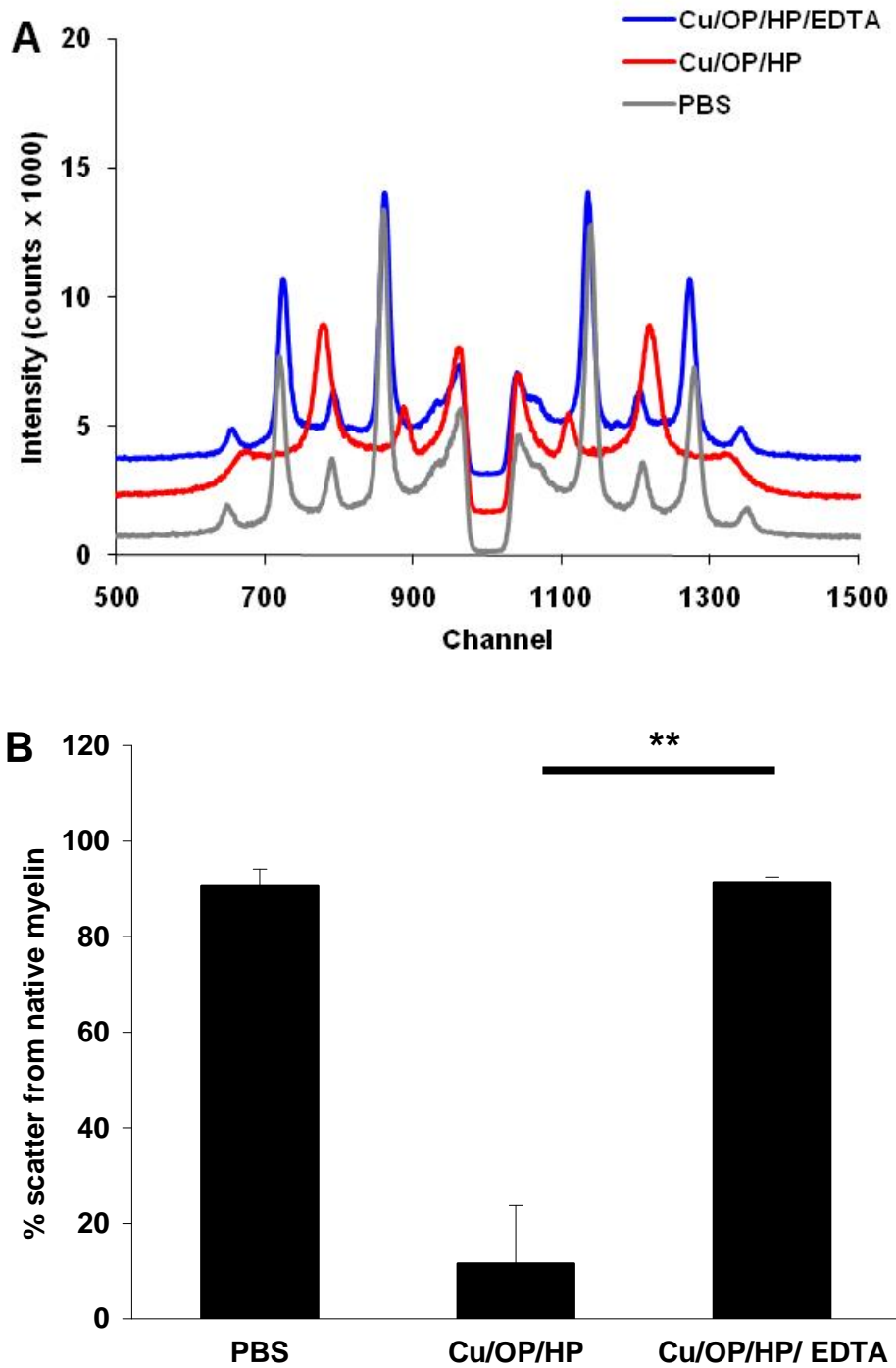


**Figure 7.** Sciatic nerve myelin from plasmalogen-deficient mice has a similar structure and stability to that from WT mice.

A. Representative XRD patterns from Pex7 KO and WT littermate control mouse sciatic nerves incubated for 72 h at RT in 20 mL of PBS (154 mM NaCl, 20 mM phosphate buffer pH 8.0). Nerves were mounted in 0.7 mm quartz capillaries filled PBS before obtaining diffraction patterns for 30 min. Patterns are shown vertically displaced from each other for enhanced clarity.

B. Scatter plot comparing the average myelin repeat period in Å and the relative amount of myelin of Pex7 KO and WT littermate control sciatic nerve myelin after incubating for 72 h at RT. Plots show the results of four experiments (WT) and three experiments (Pex7 KO). The average myelin repeat period does not differ between WT and Pex7 KO animals ( $p = 0.22$ ). Pex7 KO sciatic nerves have a slightly lower relative amount of myelin than do WT sciatic nerves ( $p = 0.045$ ).

**Figure 7.** Sciatic nerve myelin from plasmalogen-deficient mice has a similar structure and stability to that from WT mice.

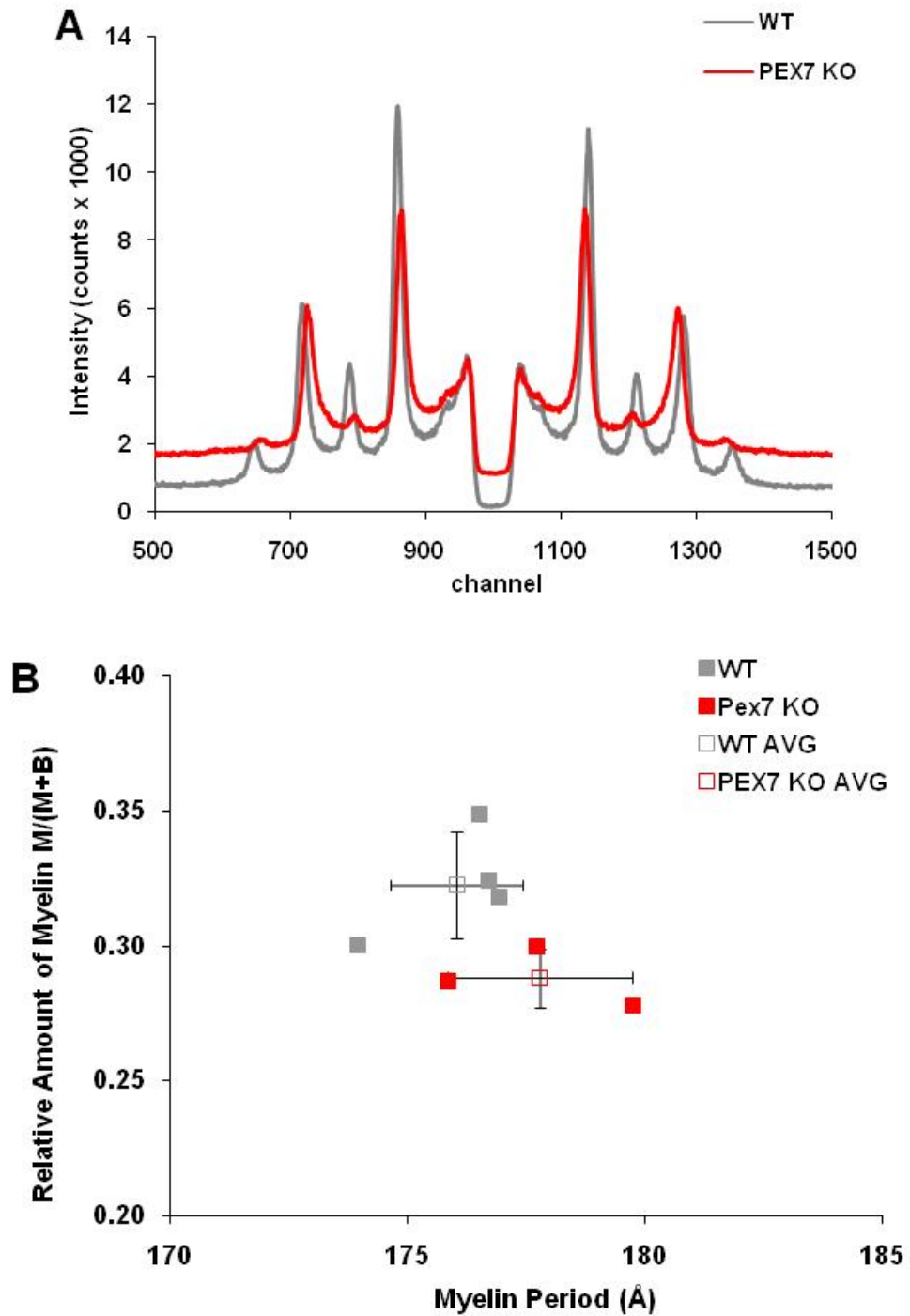


**Figure 8.** Sciatic nerve myelin from Pex7 KO mice is more vulnerable to ROS-mediated decompaction.

A. Representative XRD patterns from Pex7 KO or WT littermate control mouse sciatic nerves incubated 72 h at RT in Cu (100  $\mu$ M), OP (100  $\mu$ M), and HP (5 mM).

B. Same as in A, except that HP was at 10 mM.

C. Same as in A and B, except that HP was at 20 mM.

**Figure 8.** Sciatic nerve myelin from Pex7 KO mice is more vulnerable to ROS-mediated decompaction.

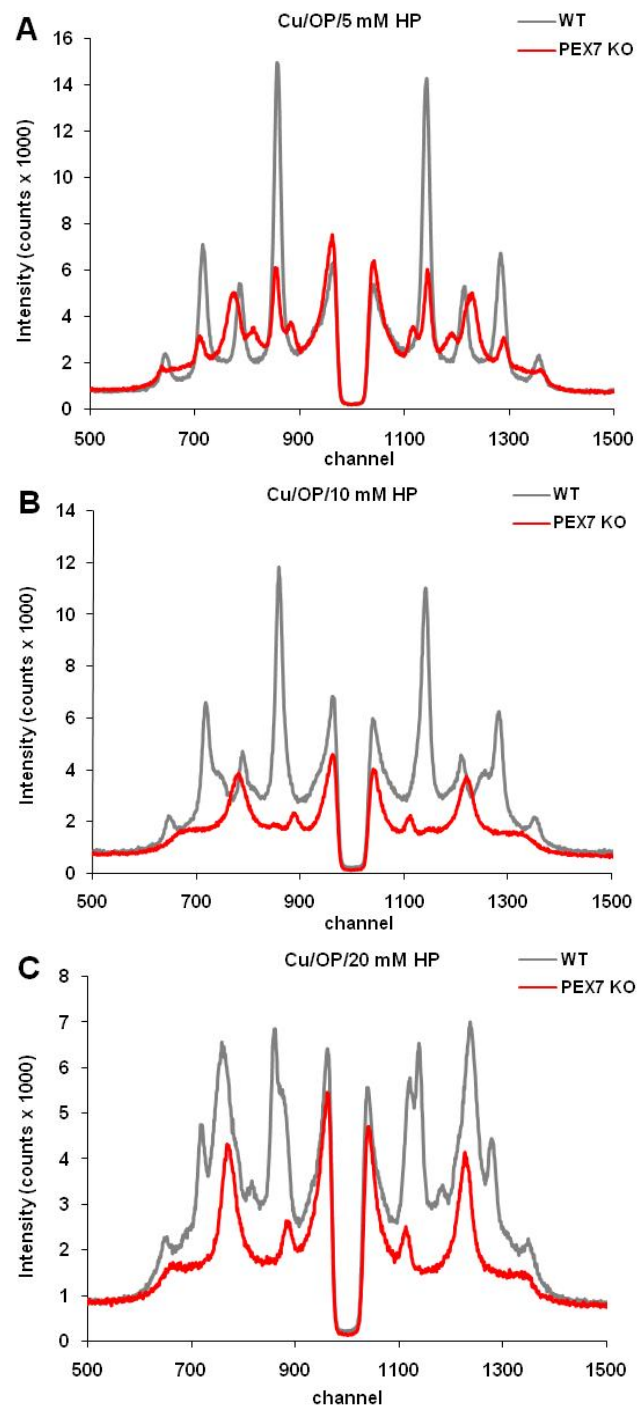




**Figure 9.** Sciatic nerve myelin from Pex7 KO mice is more vulnerable to ROS-mediated decompaction.

Quantification of x-ray scatter from myelin arrays in native, compacted state in Pex7 KO and WT littermate control mouse sciatic nerves following treatment conditions as indicated. The total scatter attributed to native myelin arrays was divided by the total scatter after background subtraction. The averages and standard deviations were calculated from four (WT, PBS), six (WT, Cu/OP/5 mM HP), seven (WT, Cu/OP/10 mM HP), four (WT, Cu/OP/ 20 mM HP), three (Pex7 KO, PBS), three (Pex7 KO, Cu/OP/5 mM HP), four (Pex7 KO, Cu/OP/10 mM HP) and one (Pex7 KO, Cu/OP/20 mM HP) separate experiments. \*  $p = 0.013$  , \*\*  $p < 0.0001$ .

**Figure 9.** Sciatic nerve myelin from Pex7 KO mice is more vulnerable to ROS-mediated decompaction.

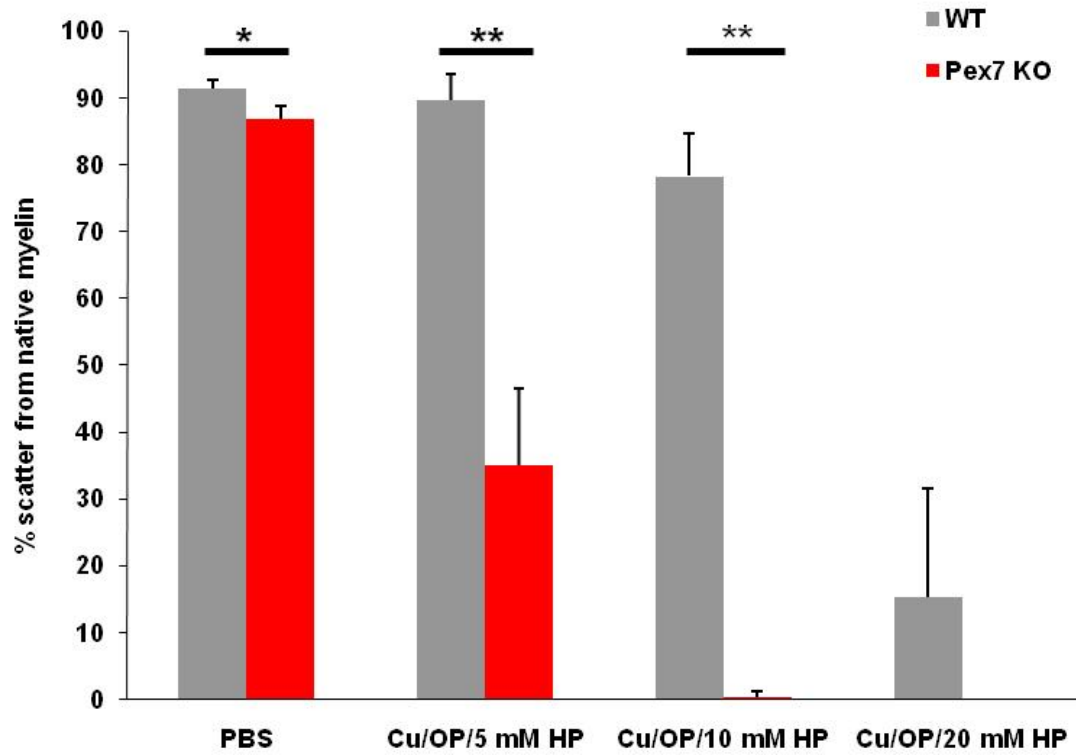


**Figure 10.** Pex7 KO sciatic nerve myelin decompaction induced by Cu/OP/HP treatment is mitigated by addition of a hydroxyl radical scavenger.

A. Representative XRD patterns from WT (littermate control) sciatic nerves incubated 72 h at RT in PBS alone, Cu (100  $\mu$ M), OP (100  $\mu$ M), and HP (20 mM), or Cu/OP/HP with sodium formate (form, 20 mM). Two patterns are shown for the Cu/OP/HP/20 mM form condition as only those two experiments were conducted. Patterns are shown vertically displaced from each other for enhanced clarity.

B. XRD patterns from Pex7 KO sciatic nerves incubated 72 h at RT in PBS alone, Cu (100  $\mu$ M), OP (100  $\mu$ M), and HP (10 mM), or Cu/OP/HP with sodium formate (form, 10 or 20 mM). Two patterns are shown for the Cu/OP/HP/20 mM form condition as only those two experiments were conducted.

**Figure 10.** Pex7 KO sciatic nerve myelin decompaction induced by Cu/OP/HP treatment is mitigated by addition of a hydroxyl radical scavenger.

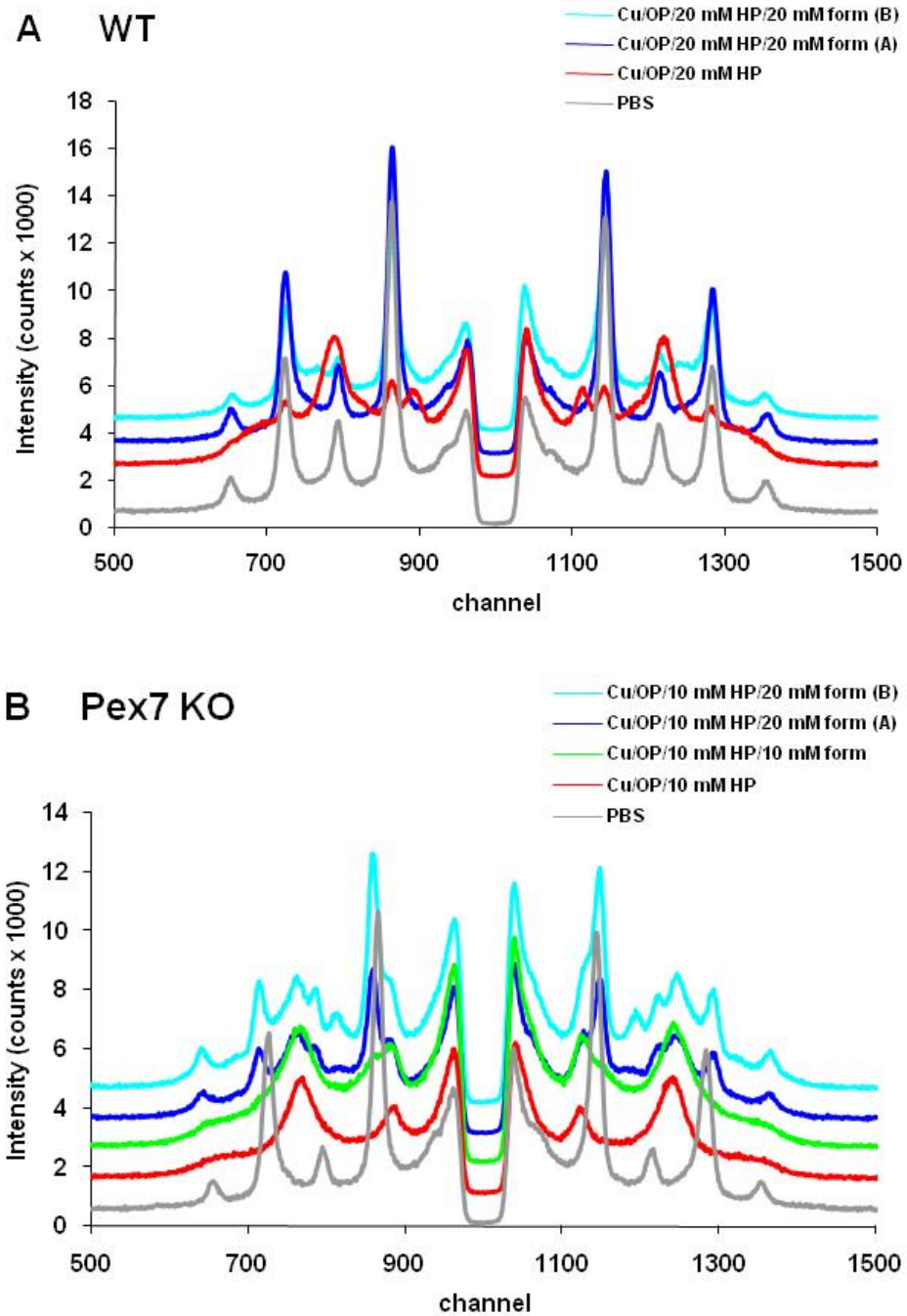


**Figure 11.** Pex7 KO sciatic nerve myelin decompaction induced by Cu/OP/HP treatment is mitigated by addition of a hydroxyl radical scavenger.

Quantification of x-ray scatter from myelin arrays in native, compacted state treated as indicated. The total scatter attributed to native myelin arrays was divided by the total scatter after background subtraction.

A. WT (littermate control) sciatic nerves were incubated 72 h at RT in PBS alone, Cu (100  $\mu$ M), OP (100  $\mu$ M), and HP (20 mM), or Cu/OP/HP with sodium formate (form, 20 mM). The averages and standard deviations were calculated from three (PBS and Cu/OP/20 mM HP) separate experiments, whereas the % scatter from native myelin was shown for two different experiments of the Cu/OP/HP 20 mM form condition.

B. Pex7 KO sciatic nerves were incubated 72 h at RT in PBS alone, Cu (100  $\mu$ M), OP (100  $\mu$ M), and HP (10 mM), or Cu/OP/HP with sodium formate (form, 10 or 20 mM).

**Figure 11.** Pex7 KO sciatic nerve myelin decompaction induced by Cu/OP/HP treatment is mitigated by addition of a hydroxyl radical scavenger.

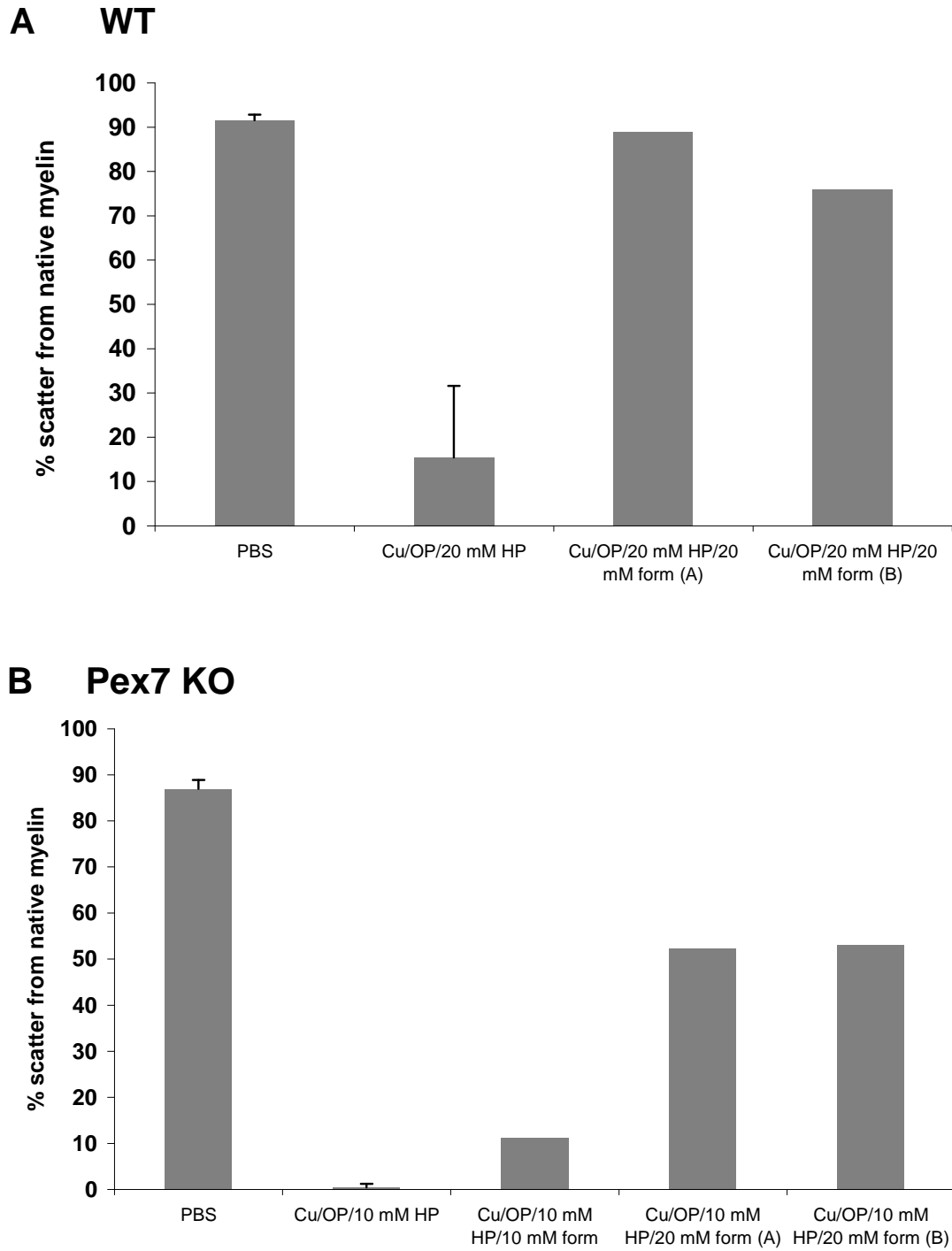


**Figure 12.** Incubation of WT optic nerves with an ROS-generating system induces irreversible myelin decompaction.

A. Representative XRD patterns from DDY mouse optic nerves incubated 24 h at RT in Cu (100  $\mu$ M), OP (100  $\mu$ M), and/or HP (20 mM). Incubations were conducted as described in materials and methods, and diffraction patterns were obtained over 60 min.

A Cu/OP/HP-treated nerve was additionally incubated in PBS for 8 hr before x-ray diffraction. Patterns are shown vertically displaced from each other for enhanced clarity

B. Quantification of x-ray scatter from myelin arrays in native, compacted state from DDY mouse optic nerves incubated as in A. The total scatter attributed to native myelin arrays was divided by the total scatter after background subtraction. The averages and/or standard deviations were calculated from two (PBS), two (Cu), one (Cu/OP), two (HP), and five (Cu/OP/HP) separate experiments.

**Figure 12.** Incubation of WT optic nerves with an ROS-generating system induces irreversible myelin decompaction.

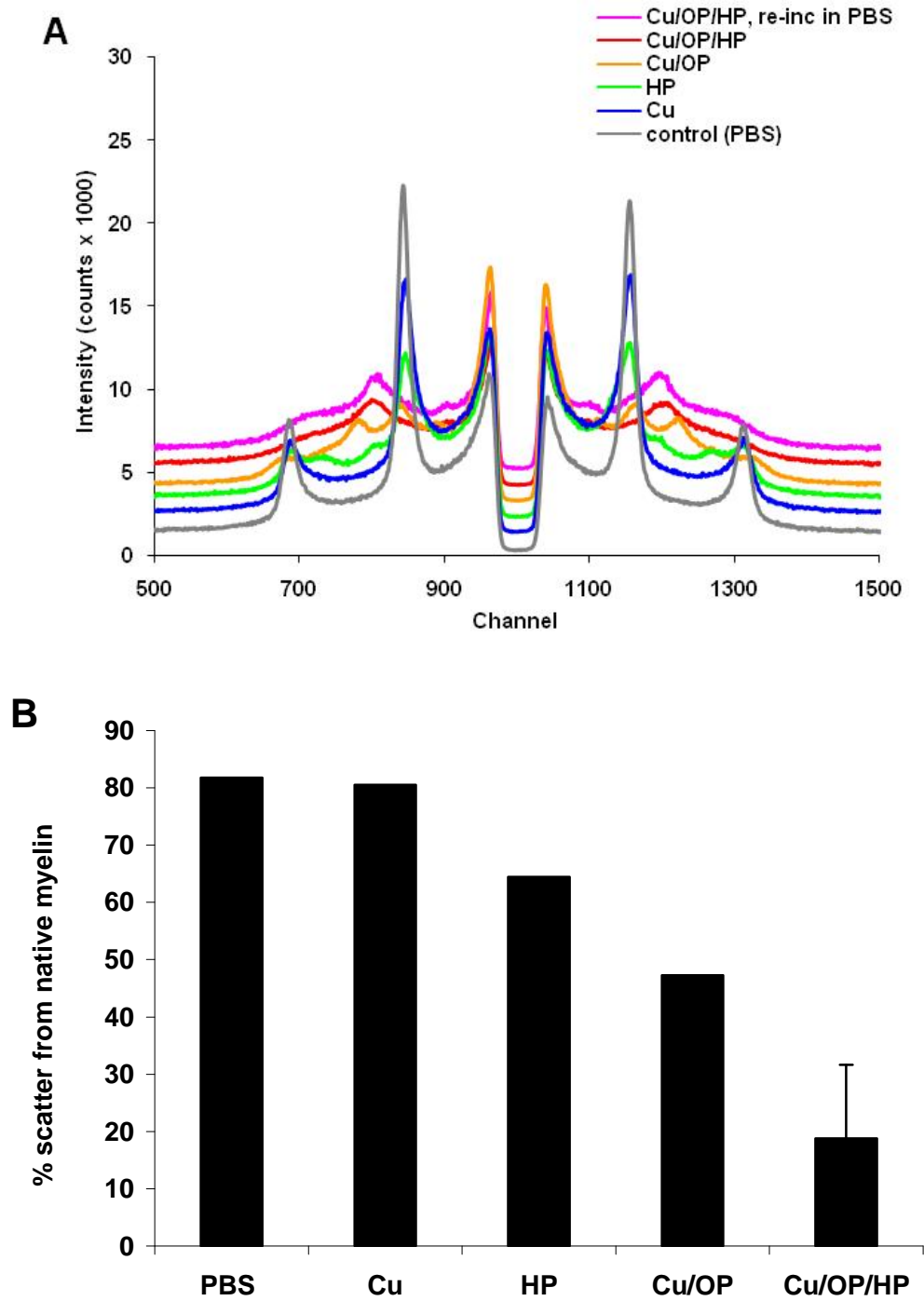
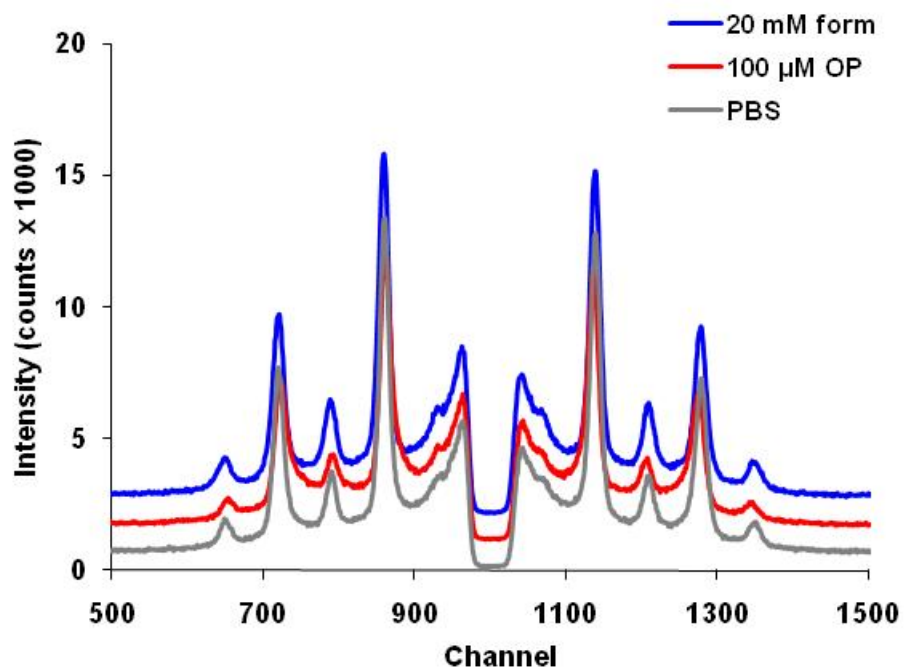




**Figure 13.** Additional sciatic nerve control experiments. Representative XRD patterns from DDY mouse sciatic nerves incubated 72 h at RT in PBS, OP (100  $\mu$ M), or formate (20 mM) as described in materials and methods. Patterns are shown vertically displaced from each other for enhanced clarity.

**Figure 13.** Additional sciatic nerve control experiments.



## References

- Avila-Carey, Robin Lee (2007). Analysis of internodal myelin structure in transgenic mice and zebrafish using X-ray diffraction. Ph.D. dissertation, Boston College, United States -- Massachusetts. Retrieved March 11, 2009, from Dissertations & Theses: Full Text database. (Publication No. AAT 3256201).
- Bartzokis, G. (2004). Age-related myelin breakdown: a developmental model of cognitive decline and Alzheimer's disease. *Neurobiology of Aging* 25, 5.
- Bongarzone, E.R., Pasquini, J.M., and Soto, E.F. (1995). Oxidative damage to proteins and lipids of CNS myelin produced by in vitro generated reactive oxygen species. *Journal of Neuroscience Research* 41, 213.
- Brites, P., Motley, A.M., Gressens, P., Mooyer, P.A.W., Ploegaert, I., Everts, V., Evrard, P., Carmeliet, P., Dewerchin, M., Schoonjans, L. *et al.* (2003). Impaired neuronal migration and endochondral ossification in Pex7 knockout mice: a model for rhizomelic chondrodysplasia punctata. *Human Molecular Genetics* 12, 2255.
- Caspar, D.L., and Kirschner, D.A. (1971). Myelin membrane structure at 10 Å resolution. *Nature: New Biology* 231, 46.
- Chan, P.C., Peller, O.G., and Kesner, L. (1982). Copper(II)-catalyzed lipid peroxidation in liposomes and erythrocyte membranes. *Lipids* 17, 331.
- Chevion, M. (1988). A site-specific mechanism for free radical induced biological damage: the essential role of redox-active transition metals. *Free Radical Biology Medicine* 5, 27.
- Engelmann, B. (2004). Plasmalogens: targets for oxidants and major lipophilic antioxidants. *Biochemical Society Transactions* 32, 147.

- Farooqui, A.A., and Horrocks, L.A. (2001). Plasmalogens: workhorse lipids of membranes in normal and injured neurons and glia. *The Neuroscientist* 7, 232.
- Fong, K.L., McCay, P.B., Poyer, J.L., Keele, B.B., and Misra, H. (1973). Evidence that peroxidation of lysosomal membranes is initiated by hydroxyl free radicals produced during flavin enzyme activity. *The Journal of Biological Chemistry* 248, 7792.
- Fridovich, S.E., and Porter, N.A. (1981). Oxidation of arachidonic acid in micelles by superoxide and hydrogen peroxide. *The Journal of Biological Chemistry* 256, 260.
- Goldstein, S., and Czapski, G. (1986). The role and mechanism of metal ions and their complexes in enhancing damage in biological systems or in protecting these systems from the toxicity of O<sub>2</sub><sup>-</sup>. *Journal of Free Radicals in Biology Medicine* 2, 3.
- Gutteridge, J.M. (1995). Lipid peroxidation and antioxidants as biomarkers of tissue damage. *Clinical Chemistry* 41, 1819.
- Gutteridge, J.M., and Halliwell, B. (1982). The role of the superoxide and hydroxyl radicals in the degradation of DNA and deoxyribose induced by a copper-phenanthroline complex. *Biochemical Pharmacology* 31, 2801.
- Gutteridge, J.M., and Wilkins, S. (1983). Copper salt-dependent hydroxyl radical formation. Damage to proteins acting as antioxidants. *Biochimica Et Biophysica Acta* 759, 38.
- Halliwell, B. (1994). Free radicals, antioxidants, and human disease: curiosity, cause, or consequence? *Lancet* 344, 721.
- Halliwell, B., and Gutteridge, J.M.C. (2007). *Free radicals in biology and medicine* (Oxford ; New York: Oxford University Press).

Huang, X., Moir, R.D., Tanzi, R.E., Bush, A.I., and Rogers, J.T. (2004). Redox-active metals, oxidative stress, and Alzheimer's disease pathology. *Annals of the New York Academy of Sciences* 1012, 153.

Inouye, H., and Kirschner, D.A. (1988). Membrane interactions in nerve myelin. I. Determination of surface charge from effects of pH and ionic strength on period. *Biophysical Journal* 53, 235.

Konat, G.W., and Wiggins, R.C. (1985). Effect of reactive oxygen species on myelin membrane proteins. *Journal of Neurochemistry* 45, 1113.

Lazzarini, R.A. (2004). *Myelin Biology and Disorders* (San Diego, Calif.: Elsevier Academic Press).

LeVine, S.M., and Wetzel, D.L. (1998). Chemical analysis of multiple sclerosis lesions by FT-IR microspectroscopy. *Free Radical Biology Medicine* 25, 33.

Lovell, M.A., Ehmann, W.D., Butler, S.M., and Markesbery, W.R. (1995). Elevated thiobarbituric acid-reactive substances and antioxidant enzyme activity in the brain in Alzheimer's disease. *Neurology* 45, 1594.

McCord, J.M., and Day, E.D. (1978). Superoxide-dependent production of hydroxyl radical catalyzed by iron-EDTA complex. *FEBS Letters* 86, 139.

McCord, J.M., and Fridovich, I. (1969). Superoxide dismutase. An enzymic function for erythrocyte hemocuprein (hemocuprein). *The Journal of Biological Chemistry* 244, 6049.

Morand, O.H., Zoeller, R.A., and Raetz, C.R. (1988). Disappearance of plasmalogens from membranes of animal cells subjected to photosensitized oxidation. *The Journal of Biological Chemistry* 263, 11597.

- Morandat, S., Bortolato, M., Anker, G., Doutheau, A., Lagarde, M., Chauvet, J., and Roux, B. (2003). Plasmalogens protect unsaturated lipids against UV-induced oxidation in monolayer. *Biochimica Et Biophysica Acta* *1616*, 137.
- Murphy, R.C. (2001). Free-radical-induced oxidation of arachidonoyl plasmalogen phospholipids: antioxidant mechanism and precursor pathway for bioactive eicosanoids. *Chemical Research in Toxicology* *14*, 463.
- Que, B.G., Downey, K.M., and So, A.G. (1980). Degradation of deoxyribonucleic acid by a 1,10-phenanthroline-copper complex: the role of hydroxyl radicals. *Biochemistry* *19*, 5987.
- Reiss, D., Beyer, K., and Engelmann, B. (1997). Delayed oxidative degradation of polyunsaturated diacyl phospholipids in the presence of plasmalogen phospholipids in vitro. *The Biochemical Journal* *323 ( Pt 3)*, 807.
- Romero, F.J. (1996). Antioxidants in peripheral nerve. *Free Radical Biology Medicine* *20*, 925.
- Samuni, A., Aronovitch, J., Godinger, D., Chevion, M., and Czapski, G. (1983). On the cytotoxicity of vitamin C and metal ions. A site-specific Fenton mechanism. *European Journal of Biochemistry* *137*, 119.
- Schaich, K.M. (1992). Metals and lipid oxidation. Contemporary issues. *Lipids* *27*, 209.
- Shapiro, L., Doyle, J.P., Hensley, P., Colman, D.R., and Hendrickson, W.A. (1996). Crystal structure of the extracellular domain from P0, the major structural protein of peripheral nerve myelin. *Neuron* *17*, 435.
- Shinar, E., Navok, T., and Chevion, M. (1983). The analogous mechanisms of enzymatic inactivation induced by ascorbate and superoxide in the presence of copper. *The Journal of Biological Chemistry* *258*, 14778.

Sindelar, P.J., Guan, Z., Dallner, G., and Ernster, L. (1999). The protective role of plasmalogens in iron-induced lipid peroxidation. *Free Radical Biology Medicine* 26, 318.

Smith, K.J., Kapoor, R., and Felts, P.A. (1999). Demyelination: the role of reactive oxygen and nitrogen species. *Brain Pathology* 9, 69.

Stadtman, E.R. (1992). Protein oxidation and aging. *Science* 257, 1220.

Stadtman, E.R. (1990). Metal ion-catalyzed oxidation of proteins: biochemical mechanism and biological consequences. *Free Radical Biology Medicine* 9, 315.

Tonkin, E.G., Valentine, H.L., Milatovic, D.M., and Valentine, W.M. (2004). N,N-diethyldithiocarbamate produces copper accumulation, lipid peroxidation, and myelin injury in rat peripheral nerve. *Toxicological Sciences* 81, 160.

Viquez, O.M., Valentine, H.L., Amarnath, K., Milatovic, D., and Valentine, W.M. (2008). Copper accumulation and lipid oxidation precede inflammation and myelin lesions in N,N-diethyldithiocarbamate peripheral myelinopathy. *Toxicology and Applied Pharmacology* 229, 77.

Zoeller, R.A., Morand, O.H., and Raetz, C.R. (1988). A possible role for plasmalogens in protecting animal cells against photosensitized killing. *The Journal of Biological Chemistry* 263, 11590.